RESEARCH PAPER
Contrib. Sci. & Tech Eng, 2026, 3(1)
Homepage: https://cste.journals.umz.ac.ir/
DOI: 10.22080/cste.2025.29155.1043

Integration of Braking-Related Vehicle Safety Systems Based on Four Wheel Independent Electro-Hydraulic Brakes

Nayereh Raesian [1]*, Hossein Gholizadeh Narm [2]

[1] *Ph.D., Electrical Engineering, Shahrood University of Technology, Shahrood, Iran.*

[2] *Associate Professor, Electrical Engineering, Shahrood University of Technology, Shahrood, Iran.*

Article Info
Received 05 May 2025
Accepted 28 September 2025
Available online 18 February 2026

Keywords:
Electro-Hydraulic Brake System;
Electronic Stability Control;
Emergency Break Assist;
Four-wheel Independent Breaking (4WIB);
Adaptive Neuro-Fuzzy Interface System (ANFIS).

Abstract:

This paper focuses on the integration of braking-related vehicle safety systems as active safety technologies, including Electronic Stability Control, Emergency Brake Assist, and Anti-lock Braking System. The proposed control system is designed using an adaptive neuro-fuzzy inference system (ANFIS) modeling approach. It accounts for seven inputs, including pedal displacement, pedal velocity, the corrective torque required to maintain vehicle stability, and the slip ratio of each of the four wheels under various dynamic and transient driving conditions. The system determines the required brake pressure for each wheel as four separate outputs to optimize braking performance. Additionally, this study considers four independent electro-hydraulic brake (EHB) control systems to achieve faster, more effective response times for each wheel, thereby enhancing safety margins during emergency maneuvers and complex cornering. The simulation results obtained with MATLAB and Carsim validate the system's performance, accuracy, and efficiency across different operational and critical scenarios.

***Corresponding Author:** n.raesian@shahroodut.ac.ir

Supplementary information: Supplementary information for this article is available at https://cste.journals.umz.ac.ir/

Please cite this paper as: Raesian, N., & Gholizadeh Narm, H. (2026). Integration of Braking-Related Vehicle Safety Systems Based on Four Wheel Independent Electro-Hydraulic Brakes. Contributions of Science and Technology for Engineering, 3(1), 52-64. doi:10.22080/cste.2025.29155.1043.

1. Introduction

Vehicle braking safety systems include standard braking during longitudinal motion, emergency braking, driver-assistance brake systems, and differential braking for vehicle stability control during cornering. They also encompass systems that prevent longitudinal slip and wheel lockup during braking under various road conditions, each requiring different algorithms to apply appropriate brake pressure to the wheels. However, having separate controls for each function in areas of overlap can lead to errors due to interference between their modes and conditions, ultimately affecting the precise pressure applied to each wheel and its priority. Therefore, a better solution is to use an integrated control system that monitors all inputs and conditions simultaneously, determining which wheel should receive how much pressure at any given time. This paper presents an integrated control system designed to maintain vehicle stability under normal, emergency, and cornering-braking conditions, while preventing wheel lockup at all times [1].

In addition, various algorithms are employed to distribute wheel pressure for braking and stability control, or to prevent wheel lockup during emergency braking. However, these algorithms can sometimes overlap or require considerable effort to generate and distribute the desired pressure promptly. This paper proposes an independent EHB system for each wheel to address these challenges.

The advantages of an independent EHB system for each wheel are as follows [2]:

1. Independent braking improves performance in bad conditions because each wheel can be controlled separately, enhancing stability and lowering the risk of skidding.

2. The system can apply more force to one wheel than the other while turning, which improves control and makes the vehicle more mobile.

3. The ability to control the brake on each wheel means that the vehicle may be faster and stop more efficiently. This capability is essential in emergencies.

The Electro-Hydraulic Brake (EHB) System is an innovative electronic braking solution (Brake-by-Wire) that replaces the traditional vacuum booster and integrates multiple functions to advance intelligent vehicle

*ISSN **3060-6578***

technologies. This system integrates key technologies, including vehicle stability control, anti-lock braking, traction control, and regenerative braking, within a unified electronic braking framework. The EHB system primarily comprises two components: a servo-motor unit and a hydraulic control unit. The permanent magnet synchronous motor (PMSM) generates high, stable pressure in the master cylinder. At the same time, the four-channel hydraulic control unit ensures precise and independent pressure modulation for each wheel cylinder [3,4].

Recent research has explored various control methods to optimize PMSM performance. One approach uses a fuzzy logic controller with direct torque control, which has been shown to enhance PMSM performance characteristics [5]. Vector control techniques have also gained traction, particularly for synchronous motor control, where a Neural Network (NN)-based vector controller demonstrates robust, adaptive performance in dynamic conditions [6, 7]. Additionally, the Direct Torque Control (DTC) method, widely used for electric motor control, has been advanced with Space Vector Modulation (SVM-DTC) to improve modulation precision and responsiveness [8]. Advanced control techniques, such as Model Predictive Control (MPC), offer significant advantages by directly tuning controllers and effectively managing constraints. To address the computational demands associated with extended prediction horizons, Nonlinear Model Predictive Control (NMPC) has been introduced as a refined approach suitable for real-time applications, providing precision with a shorter prediction horizon [9, 10]. Model Predictive Torque Control (MPTC) further improves system performance, enabling rapid response and efficient real-time operation [11].

Several robust control techniques have also been developed for PMSM regulation, including methods that ensure stability across nonlinear electric dynamics [12]. Sliding Mode Control (SMC), coupled with low-pass filtering, effectively compensates for system uncertainties, whereas combining Sliding Mode Variable Structure Control (SMVSC) with fuzzy logic yields a hybrid approach that leverages the strengths of both methods [13, 14]. Recently, Continuous Fast Terminal Sliding Mode Control (CFTSMC) has been employed for high-precision speed regulation in PMSMs [15].

Position tracking in electronic brake boosters remains a significant challenge due to the system's highly nonlinear characteristics and load-dependent friction. A proposed solution is a three-loop PI position tracking control structure [16]. Research in this area has also suggested an advanced control strategy that uses Maximum Torque per Ampere (MTPA) with adaptive current weakening to enable rapid response and precise position tracking [17]. Another notable approach employs a nonlinear control method for auxiliary braking that incorporates signal processing, driver-brake behavior detection, and accurate PMSM position control [18].

Accurate pressure control relative to the master cylinder's shaft positions is crucial for EHB systems. To this end, several adaptive controllers have been proposed. An adaptive sliding-mode hydraulic pressure controller, which relies on a hydraulic pressure estimator, aims to achieve sensorless tracking of the desired pressure [19]. Another study developed a robust adaptive controller to improve pressure tracking by incorporating a continuous friction model [20]. Additionally, Fuzzy-PI and Fuzzy control methods have been employed to regulate the hydraulic pressure of the EHB system's cylinder [21, 22]. An adaptive controller integrating fuzzy logic to dynamically adjust the weighting of a Linear Quadratic Regulator (LQR) has also been explored [23]. Furthermore, a feedforward control law for pressure tracking is designed to enhance response speed by controlling the central piston rod's position within the cylinder [24]. Incorporating dynamic vehicle stability control in EHB systems is another promising direction, with recent research highlighting hierarchical control architectures. For instance, variable-structure sliding-mode controllers within hierarchical frameworks have demonstrated potential to enhance vehicle stability [3]. A cascade controller based on a nonlinear observer was also developed for tracking cylinder pressure, effectively handling external disturbances and parameter uncertainties [24]. A three-layer stability control structure has been proposed to address dynamic vehicle instability, comprising decision-making, distribution, and execution layers, based on EHB systems [25]. Additionally, in a paper, an $H\infty$ controller is used to control the vehicle's roll angle, yielding good results [26]. Hierarchical control of ESCs has also recently attracted researchers' attention [27].

It has been implemented in a study on fuzzy and PID controllers, specifically a fuzzy sliding-mode controller, to examine the influence of these controllers on an active seat suspension system and to enhance ride comfort in a semi-trailer truck [28, 29].

Recently, four-wheel independent steering, driving, and braking (4WIS, 4WID, and 4WIB) have been adopted as actuators in various autonomous vehicles, including passenger cars [30]. The 4WIB can be regarded as an electronic stability control (ESC) that uses braking.ESC is based on a hydraulic braking system and provides independent or differential braking. The difference between 4WIB and ESC is that 4WIB uses independent electronic brakes, such as EHB and EMB. Therefore, 4WIS, 4WID, and 4WIB can improve the control performance of both human-driven and autonomous vehicles [31, 32].

In recent years, techniques such as Artificial Neural Networks (ANNs) have been widely used in control systems and to address static and dynamic challenges in the surrounding environment across different actions.

Better results will be obtained by combining two intelligent algorithms with respect to both quality and quantity. The calculations of both algorithms will be available simultaneously. The splitting of the membership function and the number of specified rules are the main complications of a fuzzy logic system. In contrast, the specification of the optimal structure and the synaptic weights are the main complications of a neural network. To address these complexities, neuro-fuzzy models are designed, neural networks are used for training to achieve the target, and fuzzy systems are used for control. ANFIS,

which combines optimization and adaptive methods, employs neural networks to enable the parameters of the membership functions in fuzzy rules to self-learn [33, 34].

In recent years, integrated systems with differential braking have been increasingly studied to improve vehicle stability. These systems employ differential braking alongside other technologies, such as active steering and active aerodynamic control, to enhance stability management [35, 36].

This paper proposes a novel ANFIS-based control system for braking-related automotive safety systems. This controller uses input variables such as the steering angle, the driver's pedal movement, braking speed (brake pedal actuation), and slip (λ), which is the difference between wheel speed and vehicle speed. In this design, the system is first modeled using data obtained from simulations of different braking modes in MATLAB and CARSIM, and then trained on a separate dataset of these data. Then, the modeled and corrected system, trained and tested with high accuracy, is integrated into the control system to manage braking-related systems. It presents a control system with objectives to maintain vehicle stability, ensure timely braking on a straight path, respond to emergency braking in curves, provide emergency brake assist, and control the ABS. Finally, it effectively generates and controls the desired pressure for each wheel using four independent EHB systems in a rapid, timely manner. ANFIS Training Parameters and model configuration are according to Table 1.

Table 1. ANFIS Parameters and Model Configuration

Parameter	Value	Description
Inputs	7	Correction torque, 4 wheel slips, brake pedal travel, and pedal speed
Outputs	4	Brake pressure for four wheels
Separate Models	4	Multi-output system implemented as separate models
Initial FIS Generation	Genfis1	
Membership	Gaussian	Used for smoothness and better convergence
Fuzzy System	Takagi-Sugeno	The output function is a linear combination of the inputs
Training Algorithm	Hybrid	Back Propagation + Least Squares
Number of Epochs	120	
samples for training	4000	
samples for testing	1000	
Error Goal	0.03	Threshold for training error convergence
Final RMSE	0.05	Root Mean Square Error on training data

2. Proposed Control System Architecture

The control architecture, as shown in Figure 1, features an ANFIS controller with 7 inputs and 4 outputs. The first input is Mc, which denotes the corrective torque required via differential braking to maintain the vehicle's path and follow the steering angle. The Mc is derived from the vehicle dynamics using the steering angle and the ESC system. The following input, x, indicates the amount of movement applied to the brake pedal by the driver or the desired braking pressure of the driver. The third input denotes pedal stroke speed, reflecting the driver's urgency to reach the desired pressure. λ represents the vehicle's slip rate, which is the difference between the vehicle speed and wheel speed. The system has 4 outputs that specify the desired pressure for each wheel at any given moment. These desired pressures are fed into the EHB control system for each wheel, and the corresponding controlled pressure is ultimately applied to each wheel.

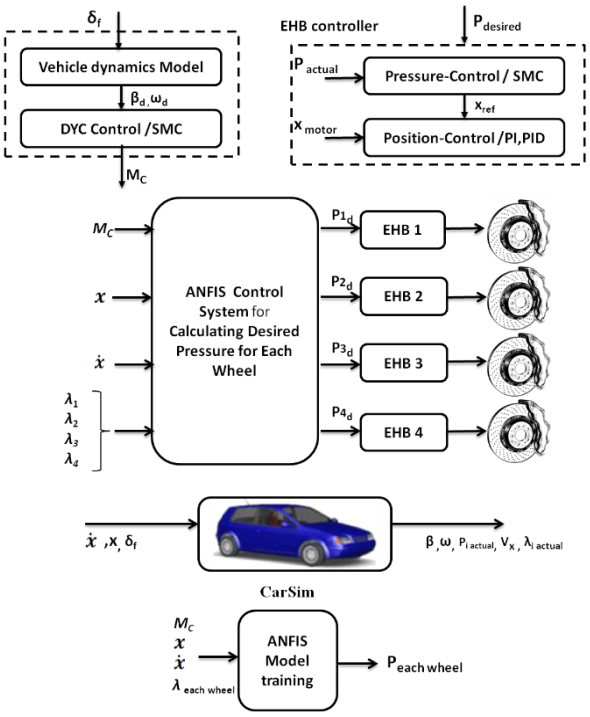

Figure 1. Proposed control system architecture

In the following sections, we will provide a detailed examination of each component that comprises this control structure.

2.1. Electric Stability Control

In this section, the required correction pressure for differential braking of the wheels is calculated based on the vehicle's deviation from the driver's steering angle input.

Figure 2 shows the four-wheel model of the car, in which the front wheels are labeled as *f* and the back wheels as *r*. R and L represent the right and left edges of the car. The center of gravity is represented by the symbol *C.G.*, while the distance from the center of gravity to the axle is labeled a, and the distance from the axle to the back is labeled *b*. L indicates the total length from the back of the car.

By assuming that both front and rear wheels are paired together, and taking the center of gravity as the origin of the coordinate system. In this model, ω_r represents the yaw rate, u denotes the longitudinal velocity, and v represents the lateral velocity.

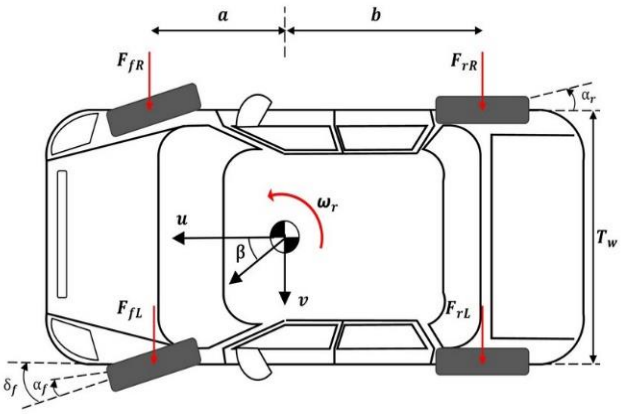

Figure 2. The vehicle model

However, in many cases, the entire vehicle model is highly complex; therefore, using a two-degree-of-freedom model is an effective approach for analyzing stability and determining the need for appropriate auxiliary torque. It enables rapid, reasonably accurate estimation of the effects of auxiliary torque by focusing on two key variables: yaw angle and lateral displacement. Additionally, models with fewer degrees of freedom require simpler calculations, which is essential in the design of controllers and active driver assistance systems, where rapid decision-making is crucial. This section is based on the two-degree-of-freedom (2-DOF) vehicle model, which serves as the reference for the car's dynamics.

If we express Newton's laws for this model, we have:

$$\sum F_y = ma_y \tag{1}$$

where m is the mass of the vehicle, and a_y is the acceleration of the vehicle in the Y-axis direction, determined by the following Equation:

$$a_y = \dot{v} + u\omega_r \tag{2}$$

In the two degrees of freedom vehicle model, F_{yf} and F_{yr} represent the lateral forces on the front and rear tires, respectively. In Figure 2, the moment of inertia around the Z-axis is denoted as I_z, and $\dot{\omega_r}$ represents the angular acceleration. By expanding and combining the aforementioned formulas, we obtain:

$$F_{yf} + F_{yr} = m(\dot{v} + u\omega_r) \tag{3}$$

$$aF_{yf} - bF_{yr} + M_c = I_z\,\dot{\omega}_r \tag{4}$$

M_c represents the corrective torque, which is the amount of torque applied to the vehicle to keep it on the desired path. If the vehicle is steered at an angle δ, we observe that the vehicle moves in the direction of a smaller angle. The difference between the steering angle δ and this angle is referred to as the tire slip angle α. The forces acting on the tires within the linear range can be expressed as follows, with coefficients α_f for the front tires and α_r for the rear tires. Additionally, β represents the vehicle's slip angle, as shown in Figure 2 [35].

$$\alpha_f = \beta + \frac{a\omega_r}{u} - \delta \tag{5}$$

$$\alpha_r = \beta - \frac{b\omega_r}{u} \tag{6}$$

For small slip angles, the tire's lateral force is directly proportional to the slip angle. This assumption can yield acceptable results in normal and mildly extreme maneuvers but may be flawed in extreme, nonlinear maneuvers, such as changes in tire stiffness.

$$F_{yf} = C_f\alpha_f \tag{7}$$

$$F_{yr} = C_r\alpha_r \tag{8}$$

C_f =80000 N/rad ±5% due to tire wear and C_r =50000 N/rad ±4% due to temperature effects, denote the lateral stiffness values for the front and rear tires, respectively.

By arranging these equations as a system and simplifying them, the vehicle dynamic state-space equations can be derived as follows:

$$\dot{\beta} = \frac{C_f+C_r}{mu}\beta + \left(\frac{aC_f-bC_r}{mu^2} - 1\right)\omega_r - \frac{C_f}{mu}\delta \tag{9}$$

$$\dot{\omega}_r = \frac{aC_f-bC_r}{I_z}\beta + \frac{a^2C_f+b^2C_r}{I_z u}\omega_r - \frac{aC_f}{I_z}\delta + \frac{1}{I_z}M_c \tag{10}$$

The goal of this controller is to ensure the vehicle's stability. This component uses internal sensor measurements to calculate the desired vehicle dynamics and the corrective torque for stability control. Thus, the desired yaw rate ω_d and lateral slip angle β_d for the vehicle's speed can be determined from the steering angle, vehicle speed, and road-tire friction coefficient [36].

In this paper, a sliding-mode controller is developed to compute the corrective torque (M_c). The sliding surface is defined as follows [37]:

$$s = \omega_r - \omega_d + \zeta(\beta - \beta_d) \tag{11}$$

Taking the derivative of the above Equation:

$$\dot{s} = \dot{\omega}_r - \dot{\omega}_d + \zeta\left(\dot{\beta} - \dot{\beta}_d\right) \tag{12}$$

As noted by Nah and Yim [31]:

$$\frac{1}{2}\frac{d}{dt}s^2 = s\dot{s} \le -\eta s^2 \tag{13}$$

And according to the dynamic Equations of the vehicle 9 to 12 , the control law will be presented as Equation 14:

$$M_c = I_z\left(\dot{\omega}_d - \eta\left(\omega_r - \omega_d + \zeta(\beta - \beta_d)\right) - \zeta(\dot{\beta} - \dot{\beta}_d)\right) - (aC_f - bC_r)\beta + \frac{a^2C_f+b^2C_r}{u}\omega_r + aC_f\delta \tag{14}$$

In this context, η and ζ are the control variables of the Sliding Mode Controller, and both are positive.

2.2. ANFIS Controller Design

Considering that the braking control system in this paper has multiple tasks, including electronic stability control, timely braking control in a straight line, anti-lock braking

control, and emergency braking control on curves and straight lines, there is a need for an integrated controller that performs the functions of each of the aforementioned controllers.

Given the complexity and nonlinearity of vehicle dynamics functions, as well as significant uncertainties, we need a robust modeling approach and a powerful controller to achieve the above control objectives. Therefore, this paper proposes ANFIS, a powerful tool for modeling vehicle dynamics and serving as a controller.

ANFIS can develop a mathematical model of the system that accurately captures its behavior. It can also be used as an intelligent controller for managing the complex braking system.

By selecting ANFIS as the system modeling and control method, we must specify the fuzzy system's inputs and outputs, along with a dataset representing these inputs and outputs.

Our model is intended to transform computable or accessible inputs into outputs, namely the desired pressure for each wheel. Therefore, seven inputs are selected as follows:

M_c: The amount of corrective torque or pressure that must be applied to the wheels to maintain vehicle stability through differential braking.

x: The amount of brake pedal displacement by the driver.

$\dot{x}$: The rate of brake pedal displacement by the driver.

λ_i: The wheel slip value, or the difference between vehicle speed and wheel speed for each wheel. (i =1…4)

Four outputs are the desired pressure for each wheel:

p_{id}: The desired pressure for each wheel. (i =1…4)

The membership functions of the inputs are defined as Gaussian, normalized, and consist of three Gaussian membership functions (L: low), (M: medium), and (H: high), characterized by two parameters: σ and c.

$$\mu_{B_j^i}(x_j) = gaussian(x_j; c, \sigma) = exp\left[-\frac{1}{2}\left(\frac{x_j - c}{\sigma}\right)^2\right] \quad (15)$$

where μ is the membership grade, c represents the center of the membership function, and σ determines its spread.

The fuzzy system is of the Takagi-Sugeno type, and the outputs are crisp. Each rule is expressed as a linear combination of inputs, yielding an output of the fuzzy control system represented as a weighted average.

Using data from various braking scenarios in real-world conditions or software simulations like CarSim, and performing calculations under different conditions, input and output data are obtained. The input and output data are used to train the base fuzzy system, yielding a modified system relative to the defined base system. Figure 3 shows the inputs and their modified values after training.

After training and testing, the new fuzzy control system is ready to be deployed as the central control system to appropriately control the outputs in response to changes in the latest input data.

2.3. Four-Wheel Independent Braking

This paper proposes using four electro-hydraulic braking systems (one for each wheel) instead of a single central electro-hydraulic system. Employing four independent pressure control systems offers several advantages:

1. Independent wheel control allows for applying greater force and pressure to specific wheels, which can improve enhanced stability and reduce the risk of losing control.

2. The vehicle can stop faster and more effectively in adverse conditions so improved stopping performance.

3. Independent control enables a quicker reduction in pressure upon wheel lock-up, preventing the wheel from locking and optimizing the Anti-Lock braking system function.

Of course, using 4 independent pressure control systems can have disadvantages, including increased costs, which can be overlooked given the great importance of safety.

The control structure of the electro-hydraulic brake (EHB) is explained in the next section.

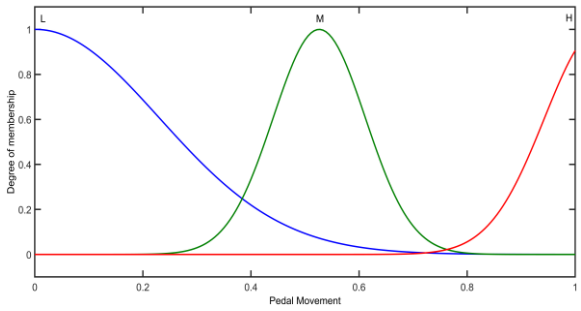

(a)

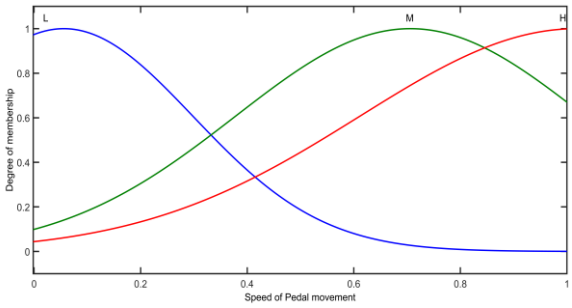

(b)

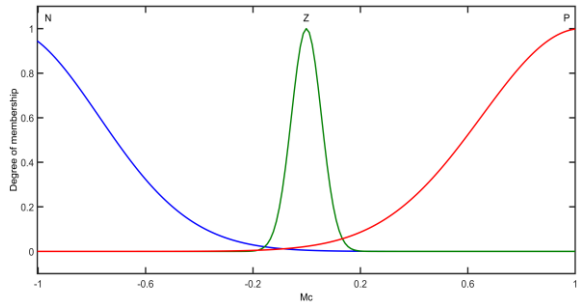

(c)

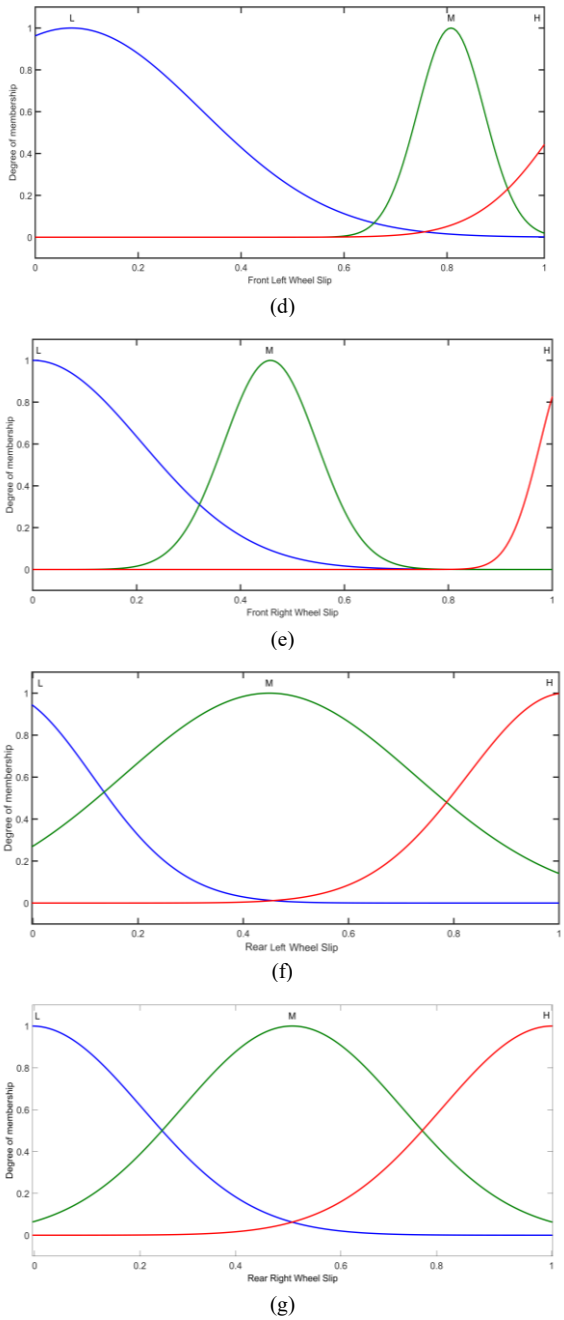

Figure 3. Membership functions of the inputs after training (a) pedal movement, (b) pedal speed, (c) M_c, (d) front-left wheel slip, (e) front-right wheel slip ,(f) rear-left wheel slip ,(g) rear-right wheel slip

2.4. EHB Braking System

Unlike traditional hydraulic brakes, there is no mechanical linkage between the brake pedal and the master cylinder in the electro-hydraulic brake system. In addition, the driver's desired braking pressure is sent electronically. When the brakes are installed, a measuring sensor accurately assesses their position and applies the appropriate electronic command to the actuator to ensure effective braking performance.

To determine the motor position required to generate brake pressure in the EHB system, effective pressure control and position control are essential. A double closed-loop controller with a cascaded structure is employed to regulate the PMSM motor position based on the required wheel pressure. This configuration comprises an external loop that controls the master cylinder pressure and an internal loop that controls the rack position.

The objective of this cascaded dual-loop controller is to manage external pressure by generating a signal for the desired position, x_{ref}, tailored explicitly for the inner controller.In the outer pressure loop, an x_{ref} virtual control is implemented as the command input to the inner position control loop. This configuration allows the internal-state bandwidth to respond faster than the external-pressure loop, thereby enabling prompt addressing of disturbances caused by nonlinearity and inherent system uncertainties [38].

2.4.1. Pressure Control

In this paper, to According to author's previous study by Montani et al. [39], the relationship between pressure and position is modeled by a simple second-order polynomial as follows:

$$p = 0.381x^2 \tag{16}$$

By calculating the time derivative of p, we can get

$$\dot{p} = 2 * 0.381x\dot{x} \tag{17}$$

This way, the sliding surface is defined.

$$s = p - \dot{p} + k_0\sigma = p - p_\sigma \tag{18}$$

$$\dot{\sigma} = -k_0\sigma + \varepsilon sat\left(\frac{s}{\varepsilon}\right), |\sigma(0)| \leq \frac{\varepsilon}{k_0} \tag{19}$$

The time derivative s can be obtained as follows by inserting it into the above Equation:

$$\dot{s} = \dot{\tilde{p}} + k_0\dot{\sigma} = a_1\dot{p}x + a_2\dot{p} - \dot{p}_d + k_0\dot{\sigma} \tag{20}$$

So x_d controller for x is designed as follows:

$$x_d = \frac{1}{a_1\dot{p}}\left[\dot{p}_d - a_2\dot{p} - k_0\dot{\sigma} - c_1 s - c_2 sat\left(\frac{s}{\varepsilon}\right)\right] \tag{21}$$

where in $a_1 < 0, a_2 > 0$, In which c_1 and c_2 are both constant and in this paper c_1=c_2=4.5e^{-4} [36].

2.4.2. Position Control

This paper uses a dual-layer control architecture for a Permanent Magnet Synchronous Motor (PMSM) driven by a three-phase inverter. The inner loop is governed by two proportional-integral (PI) controllers that regulate current, while the outer loop employs two proportional-integral-derivative (PID) controllers to manage speed and position.

The output of the position controller serves as the reference for the speed controller, with the speed controller's output acting as the reference for the q-axis current controller. The d-axis current reference is maintained at zero. The system measures the PMSM's position and currents. Velocity is obtained by taking the derivative of the position data. The PID controller outputs are produced on the *dq*-axis and then

applied to the three-phase PMSM through inverse park conversion [40].

In this paper, four EHB control systems are considered as shown in Figure 1.The output of each EHB controller is the desired pressure generated by the pressure control system through each master cylinder. This pressure is then applied to the corresponding wheel.

3. Simulation Result and Analysis

To closely replicate fundamental vehicle dynamics, the CARSIM [41] model has been employed, providing precise, detailed, and efficient methods for simulating vehicle performance. This approach includes MATLAB simulations of the EHB system and of other integrated control systems. MATLAB is used to simulate the PMSM, implement the master cylinder system, and model the caliper and wheel components. The mechanical aspects of the EHB braking system are also simulated in MATLAB [42]. Vehicle parameters are set according to Table 2.

Table 2. Vehicle parameters

Parameter	value	Description
m	1231 kg	Vehicle total mass
m_s	1111 kg	Vehicle sprung mass
l	2.6 m	Longitudinal wheel base
a	1.04 m	Distance of c.g. from front axle
b	1.56 m	Distance of c.g. from rear axle
I_z	2031.4 kg.m^2	Yaw inertia of the vehicle
R	0.3 m	Tire radius
h_{cg}	0.54 m	Height of c.g. of the vehicle
T_w	1.33 m	Vehicle body width

As discussed in Section 2, the proposed controller architecture is designed to achieve the following three objectives:

1- Electric stability control

2- Anti-lock braking control

3- Emergency brake assist

Therefore, we evaluate the system performance with three approaches:

3.1. ESC System Evaluation

As mentioned earlier, in the proposed control structure, vehicle stability control is achieved by calculating the required correction torque (MC) and applying it as braking pressure to the wheels via differential braking. In the proposed structure, the calculated correction torque is used as input to the fuzzy controller, and the appropriate pressure output for each wheel is obtained from the fuzzy controller, which has been previously trained with proper data. It is then applied to each wheel in a controlled manner via the wheel's EHB controller.

In this research, it is assumed that the pressure of each wheel can be measured with a sensor.

In this experiment, we evaluate the effectiveness of the ESC system. To assess the proposed control system, we conduct steering experiments. During these tests, the steering angle is set to 300 degrees in step mode.

Figure 4 illustrates the required pressure for each wheel to maintain stability during fishhook steering maneuvers, as shown in Figure 5. As shown, the system presented in this paper responds more quickly and applies higher pressures than a non-integrated ESC system that uses a common EHB controller for all four wheels. As a result, it performs better in reducing yaw rate, as shown in Figure 6.

3.2. EBA System Evaluation

The EBA system is designed to increase braking force in emergencies by detecting emergencies based on the rate at which the brake pedal is pressed.

In this section, the response of the proposed control system will be examined by simulating a rapid braking as shown in Figure 7.

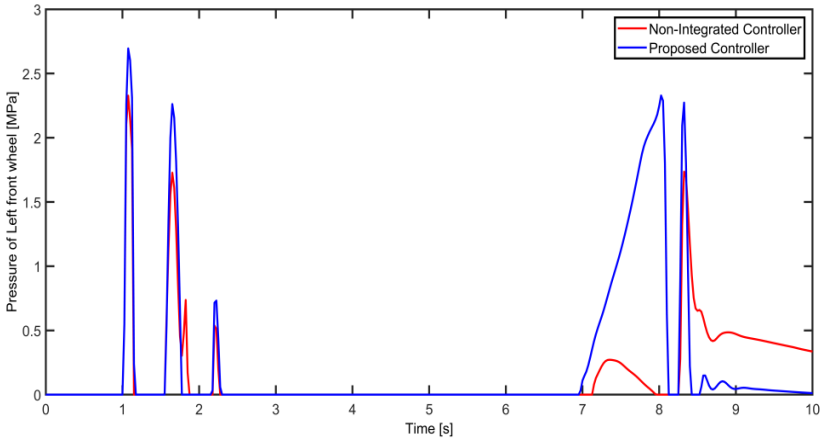

(a)

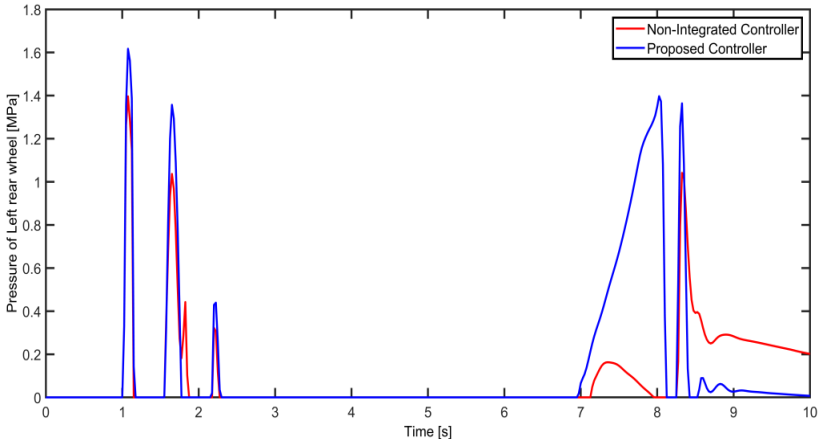

(b)

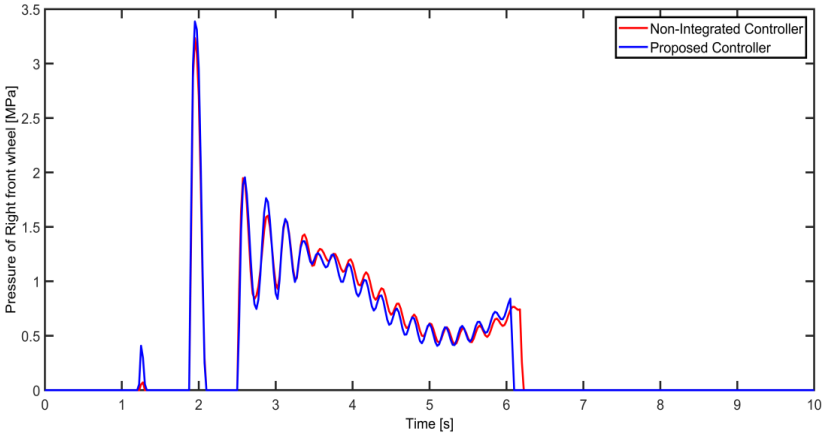

(c)

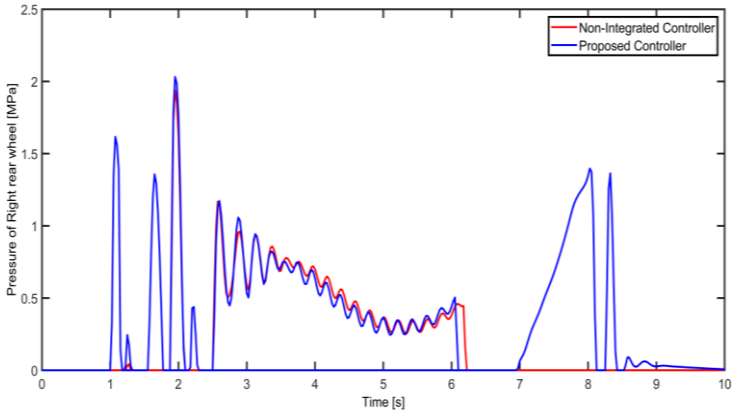

(d)

Figure 4. **Pressure on each wheel in fishhook steering test (a) left-front, (b) left -rear, (c) right-front, (d) right-rear**

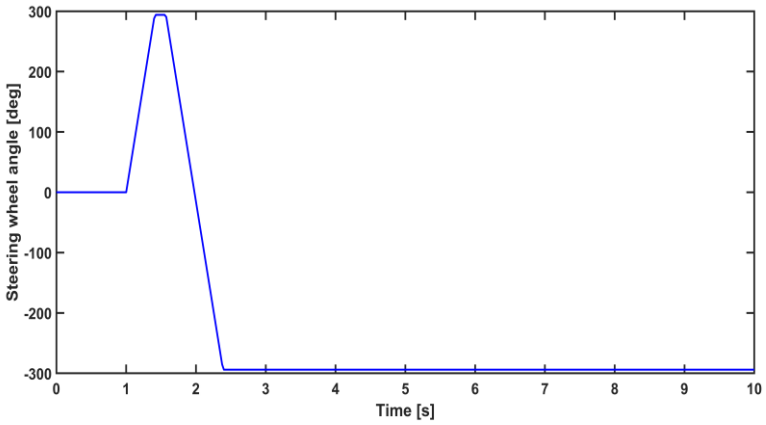

Figure 5. **Fishhook steering test**

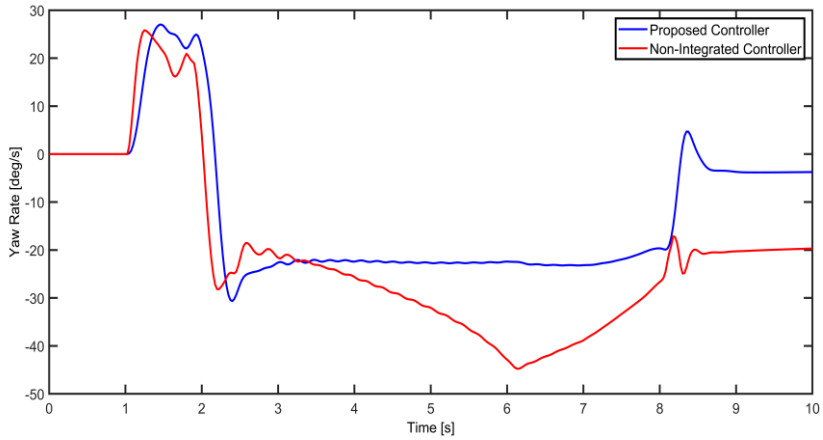

Figure 6. **Yaw rate in fishhook steering test**

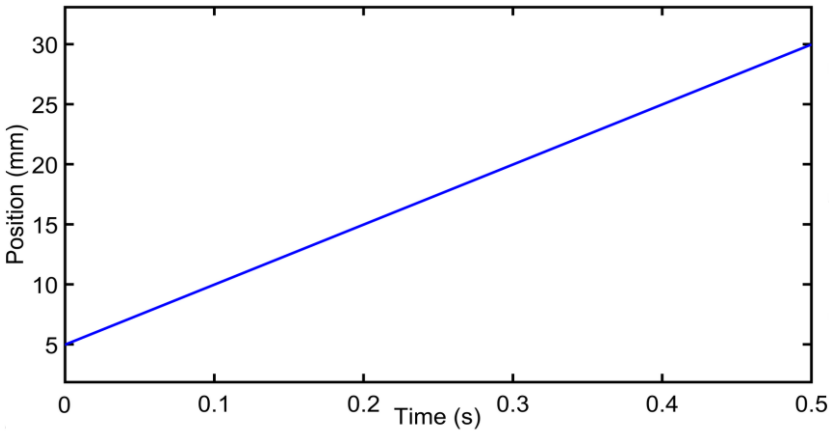

Figure 7. **Pedal movement**

For comparison, the emergency brake assist control system will be deactivated first, and then the wheel output pressure will be analyzed. As seen in Figure 8, the pressure begins to increase at a particular slope and reaches its maximum value in approximately 1.6 seconds. This maximum value is slightly higher on the front wheels than on the rear wheels.

Accordingly, the proposed control system activates the emergency braking system. The results show that the control system reaches maximum wheel pressure in approximately 0.3 seconds, as illustrated in Figure 9, indicating correct operation.

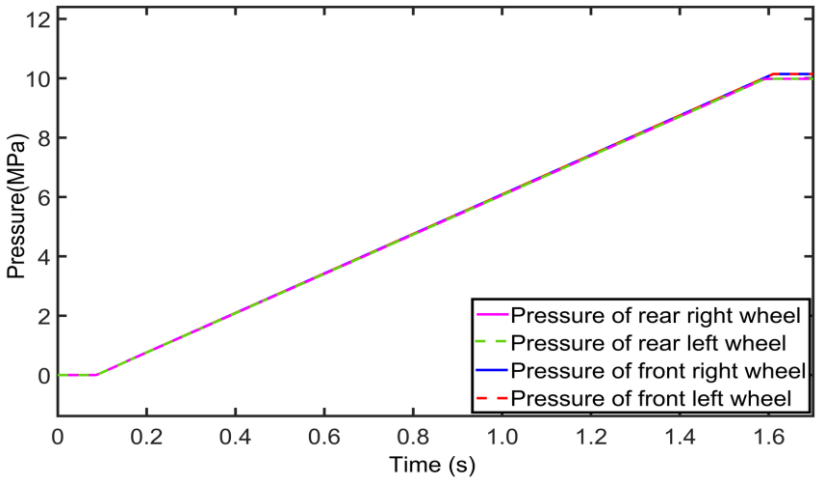

Figure 8. **Pressure of each wheel in Normal Braking**

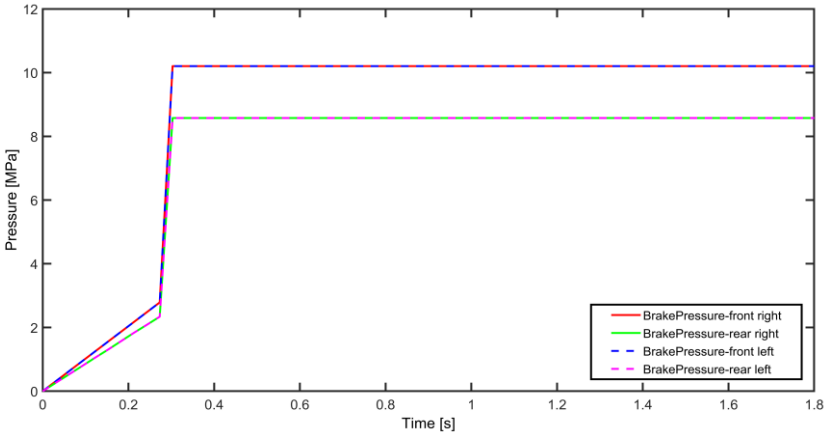

Figure 9. **Pressure of each wheel in Emergency Braking**

3.3. ABS Evaluation

In Figure 10, the wheel speeds and their differences from the vehicle speed (slip rate) are shown when the ABS control system is deactivated. This figure reveals a significant discrepancy between the vehicle speed and the wheel speeds, with one of the wheels (front-left) dropping to nearly zero at times, indicating wheel lock.

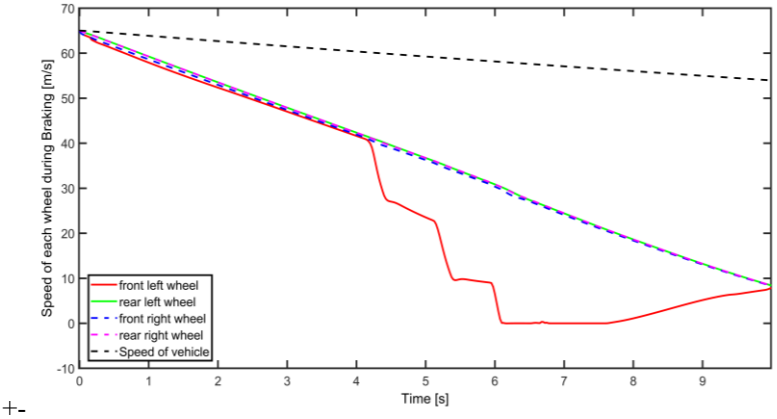

Figure 10. **Speed of each wheel When the ABS control system is deactivated**

Figure 11 illustrates the wheel speeds and the vehicle speed when the proposed ABS control system is active. As seen in the figure, under the testing and steering maneuvering conditions depicted in fig. 4, the vehicle's speed and the speeds of all four wheels are nearly equal, indicating satisfactory results.

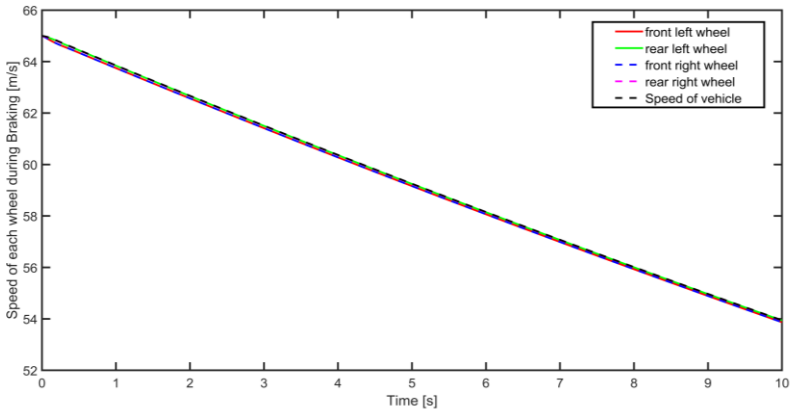

Figure 11. **Speed of each wheel When the ABS control system is activated**

Figure 12 also shows the slip ratios of all four wheels when the ABS control system is deactivated. As observed, the variations are high, reaching up to 1.2.

When the proposed ABS control system is activated, the wheel slip rates are shown in Figure 13. The significant reduction observed (maximum 0.16) indicates a satisfactory result

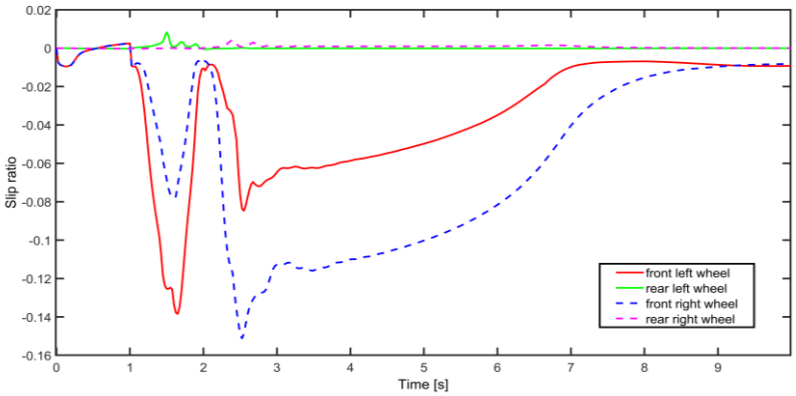

Figure 12. Slip ratio of each wheel when the ABS control system is deactivated

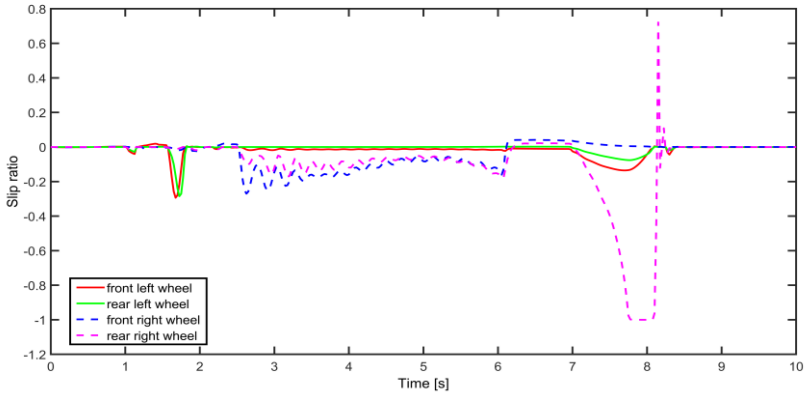

Figure 13. Slip ratio of each wheel when the ABS control system is activated

4. Conclusion

Today, most vehicles are equipped with ESC systems based on differential braking, ABS, or EBA. These features provide good support for driver safety. However, these assist systems can conflict during braking. For instance, in a sharp turn where the stability control system is activated, an emergency braking situation might arise. This raises a critical and challenging issue: should the priority be maintaining vehicle stability, drastically reducing speed, or preventing wheel lockup.

This paper proposes a comprehensive ANFIS-based system to address this challenge by leveraging accurate training data. The system receives seven inputs at any given time, including corrective torque, pedal movement, pedal movement speed, and slip from all four wheels, and continuously calculates the optimal pressure for each wheel. Additionally, to apply these pressures more swiftly and effectively for each wheel, an independent EHB control system is implemented. Results demonstrate that the proposed system effectively meets the defined needs with satisfactory performance.

The use of multiple pressure control systems can, in some cases, improve stability and reliability. However, the use of four independent pressure control systems can entail disadvantages, including increased costs, which may be overlooked given the high importance of safety. Real-time implementation means that the system responds to commands and sensor inputs almost instantaneously, allowing immediate adjustments to braking pressure based on driving conditions.

To evaluate the performance of the proposed method, the obtained results were compared with those presented in the benchmark paper [43]. In the study mentioned, MPC-based ESC was used for vehicle stability control. By comparing the yaw rate with that reported in the paper, it is observed that, due to the smaller steering angle (200 deg) compared to the proposed paper, the yaw rate has significantly improved. Additionally, compared with a similar article that used an integrated EHB system for four wheels under the same test conditions, the system with 4 independent EHB systems showed a significant improvement. When emergency braking is activated, pressure is applied to all four wheels much faster than in reference number [44], which is substantial and indicates much faster braking with an independent electro-hydraulic brake system for each wheel. Under the same test conditions, pressure reaches the wheels approximately 1 second earlier.

In this paper, the feasibility of simultaneous control of ESC and Emergency braking for vehicle stability control and rapid speed reduction in emergencies is explored theoretically. The proposed method is verified through software-in-the-loop (SIL) testing, which differs from hardware-in-the-loop (HIL) and real-world driving experiments, in that it does not account for signal disturbances or delays. To this end, the proposed method will be implemented on a HIL platform and in a prototype vehicle in the future.

5. References

[1] Lutanto, A., Fajri, A., Cikal Nugroho, K., & Falah, F. (2025). Advancements in Automotive Braking Technology for Enhanced Safety: A Review. Multidisciplinary Innovations and Research in Applied Engineering, 1(1), 6–21. doi:10.70935/6n21wx31.

[2] Park, M., & Yim, S. (2025). Design of Static Output Feedback Integrated Path Tracking Controller for Autonomous Vehicles. Processes, 13(5), 1335. doi:10.3390/pr13051335.

[3] He, X., Yang, K., Ji, X., Liu, Y., & Deng, W. (2017). Research on Vehicle Stability Control Strategy Based on Integrated-Electro-Hydraulic Brake System. SAE Technical Paper Series, 1. doi:10.4271/2017-01-1565.

[4] Ajami, M., Jannat, H., & Masih-Tehrani, M. (2020). The Effect of Tire Pressure Changes on Braking Efficiency and Necessity of Adjusting Tire Pressure Before Braking Test at Vehicle Technical Inspection Centers. Automotive Science and Engineering, 10(4), 3446–3456. doi:10.22068/ijae.10.4.3446.

[5] Gaddam, T. R. Das, & Danduprolu, K. K. (2019). Fuzzy logic controller based performance of SPMSM fed with improved direct torque control. International Journal of Renewable Energy Research, 9(3), 1346–1354. doi:10.20508/ijrer.v9i3.9625.g7714.

[6] Bida, V. M., Samokhvalov, D. V., & Al-Mahturi, F. Sh. (2018). PMSM vector control techniques — A survey. 2018 IEEE Conference of Russian Young Researchers in Electrical and Electronic Engineering (EIConRus), 577–581. doi:10.1109/eiconrus.2018.8317164.

[7] Li, S., Won, H., Fu, X., Fairbank, M., Wunsch, D. C., & Alonso, E. (2020). Neural-Network Vector Controller for Permanent-Magnet Synchronous Motor Drives: Simulated and Hardware-Validated Results. IEEE Transactions on Cybernetics, 50(7), 3218–3230. doi:10.1109/TCYB.2019.2897653.

[8] Wang, X., Wang, Z., & Xu, Z. (2019). A hybrid direct torque control scheme for dual three-phase PMSM drives with improved operation performance. IEEE Transactions on Power Electronics, 34(2), 1622–1634. doi:10.1109/TPEL.2018.2835454.

[9] Mynar, Z., Vesely, L., & Vaclavek, P. (2016). PMSM Model Predictive Control with Field-Weakening Implementation. IEEE Transactions on Industrial Electronics, 63(8), 5156–5166. doi:10.1109/TIE.2016.2558165.

[10] Younesi, A., Tohidi, S., & Feyzi, M. R. (2018). Improved optimization process for nonlinear model predictive control of PMSM. Iranian Journal of Electrical and Electronic Engineering, 14(3), 278–288. doi:10.22068/IJEEE.14.3.278.

[11] Luo, Y., & Liu, C. (2018). A simplified model predictive control for a dual three-phase PMSM with reduced harmonic currents. IEEE Transactions on Industrial Electronics, 65(11), 9079–9089. doi:10.1109/TIE.2018.2814013.

[12] Mendoza-Mondragon, F., Hernandez-Guzman, V. M., & Rodriguez-Resendiz, J. (2018). Robust Speed Control of Permanent Magnet Synchronous Motors Using Two-Degrees-of-Freedom Control. IEEE Transactions on Industrial Electronics, 65(8), 6099–6108. doi:10.1109/TIE.2017.2786203.

[13] Zhao, Y., & Dong, L. (2019). Robust current and speed control of a permanent magnet synchronous motor using SMC and ADRC. Control Theory and Technology, 17(2), 190–199. doi:10.1007/s11768-019-8084-y.

[14] Mo, L., Liu, Y., & Zhang, Y. (2019). Sliding Mode Variable Structure Control for Surface Permanent Magnet Synchronous Motors Based on a Fuzzy Exponential Reaching Law. Mathematical Problems in Engineering, 2019(1). doi:10.1155/2019/8340956.

[15] Xu, W., Junejo, A. K., Liu, Y., & Islam, M. R. (2019). Improved Continuous Fast Terminal Sliding Mode Control with Extended State Observer for Speed Regulation of PMSM Drive System. IEEE Transactions on Vehicular Technology, 68(11), 10465–10476. doi:10.1109/TVT.2019.2926316.

[16] Chen, P., Wu, J., Zhao, J., He, R., Liu, H., & Zhang, K. (2018). Design and Position Control of a Novel Electric Brake Booster. SAE International Journal of Passenger Cars - Mechanical Systems, 11(5), 389–400. doi:10.4271/2018-01-0812.

[17] Zhang, H., Wu, J., He, R., & Chen, Z. (2019). Development and Verification of Control Algorithm for Permanent Magnet Synchronous Motor of the Electro-Mechanical Brake Booster. SAE Technical Paper Series, 1. doi:10.4271/2019-01-1105.

[18] Chen, P., Wu, J., Zhao, J., He, R., Liu, H., & Yang, C. (2018). Design and Power-Assisted Braking Control of a Novel Electromechanical Brake Booster. SAE International Journal of Passenger Cars - Electronic and Electrical Systems, 11(3), 171–181,. doi:10.4271/2018-01-0762.

[19] Han, W., Xiong, L., & Yu, Z. (2019). Braking pressure control in electro-hydraulic brake system based on pressure estimation with nonlinearities and uncertainties. Mechanical Systems and Signal Processing, 131, 703–727. doi:10.1016/j.ymssp.2019.02.009.

[20] Ji, Y., Zhang, J., He, C., Ma, R., Hou, X., & Hu, H. (2022). Constraint performance pressure tracking control with asymmetric continuous friction compensation for booster based brake-by-wire system. Mechanical Systems and Signal Processing, 174, 109083. doi:10.1016/j.ymssp.2022.109083.

[21] Chen, Q., Shao, H., Liu, Y., Xiao, Y., Wang, N., & Shu, Q. (2020). Hydraulic-pressure-following control of an electronic hydraulic brake system based on a fuzzy proportional and integral controller. Engineering Applications of Computational Fluid Mechanics, 14(1), 1228–1236. doi:10.1080/19942060.2020.1816495.

[22] Soliman, A. M. E., Kaldas, M. M., Soliman, A. M. A., & Huzayyin, A. S. (2024). Vehicle Braking Performance Improvement via Electronic Brake Booster. SAE International Journal of Vehicle Dynamics, Stability, and NVH, 8(1). doi:10.4271/10-08-01-0005.

[23] Gao, Z., Yang, Y., Chen, G., Yuan, L., Zhou, J., & Zhang, J. (2022). Adaptative Pressure Estimation and Control Architecture for Integrated Electro-Hydraulic Brake System. doi:10.21203/rs.3.rs-1793406/v1.

[24] Han, W., Xiong, L., & Yu, Z. (2018). Braking Pressure Tracking Control of a Pressure Sensor Unequipped Electro-Hydraulic Booster Based on a Nonlinear Observer. SAE Technical Paper Series, 1. doi:10.4271/2018-01-0581.

[25] Lao, D., Wu, J., He, R., Zhu, B., Zhao, J., & Chen, Z. (2020). Research on Yaw Stability Control of Unmanned Vehicle Based on Integrated Electromechanical Brake Booster. SAE Technical Paper Series, 1. doi:10.4271/2020-01-0212.

[26] Nazemi, S., Masih-Tehrani, M., & Mollajafari, M. (2022). GA tuned H∞ roll acceleration controller based on series active variable geometry suspension on rough roads. International Journal of Vehicle Performance, 8(2–3), 166–187. doi:10.1504/IJVP.2022.122047.

[27] Bartfai, A., Voros, I., & Takacs, D. (2023). Stability analysis of a digital hierarchical steering controller of autonomous vehicles with multiple time delays. Journal of Vibration and Control, 30(1–2), 330–341. doi:10.1177/10775463221146624.

[28] Gheibollahi, H., Tehrani, M. M., & Najafi, A. (2024). Improving ride comfort approach by fuzzy and genetic-based PID controller in active seat suspension. International Journal of Automation and Control, 18(2), 184–213. doi:10.1504/ijaac.2024.137072.

[29] Najafi, A., Masih-Tehrani, M., Emami, A., & Esfahanian, M. (2022). A modern multidimensional fuzzy sliding mode controller for a series active variable geometry suspension. Journal of the Brazilian Society of Mechanical Sciences and Engineering, 44(9), 425. doi:10.1007/s40430-022-03735-0.

[30] Jeong, Y., & Yim, S. (2021). Model predictive control-based integrated path tracking and velocity control for autonomous vehicle with four-wheel independent steering and driving. Electronics (Switzerland), 10(22), 2812. doi:10.3390/electronics10222812.

[31] Nah, J., & Yim, S. (2020). Vehicle stability control with four-wheel independent braking, drive and steering on in-wheel motor-driven electric vehicles. Electronics (Switzerland), 9(11), 1–16. doi:10.3390/electronics9111934.

[32] Jeong, Y., & Yim, S. (2022). Path Tracking Control With Four-Wheel Independent Steering, Driving and Braking Systems for Autonomous Electric Vehicles. IEEE Access, 10, 74733–74746. doi:10.1109/access.2022.3190955.

[33] Saleh, M. S., Al Mashhadany, Y., Alshaibi, M., Ameen, F. M., & Algburi, S. (2025). Optimal Mobile Robot Navigation for Obstacle Avoidance Based on ANFIS Controller. Journal of Robotics and Control (JRC), 6(1), 484–492. doi:10.18196/jrc.v6i1.24882.

[34] Tang, W., Jiao, X., & Zhang, Y. (2025). Hierarchical energy management control for connected hybrid electric vehicles in uncertain traffic scenarios. Energy, 315, 134291. doi:10.1016/j.energy.2024.134291.

[35] Mirzaeinejad, H., Mirzaei, M., & Rafatnia, S. (2018). A novel technique for optimal integration of active steering and differential braking with estimation to improve vehicle directional stability. ISA Transactions, 80, 513–527. doi:10.1016/j.isatra.2018.05.019.

[36] Huang, Z., & Wu, Y. (2015). Lane departure Assistance based on balanced longitudinal slip ratio differential braking control. International Journal of Vehicle Safety, 8(3), 205–217. doi:10.1504/IJVS.2015.070767.

[37] Chen, Z., Wu, Y., & Li, F. (2020). Integrated Control of Differential Braking and Active Aerodynamic Control for Improving High Speed Stability of Vehicles. International Journal of Automotive Technology, 21(1), 61–70. doi:10.1007/s12239-020-0007-x.

[38] Han, W., Xiong, L., & Yu, Z. (2020). Interconnected Pressure Estimation and Double Closed-Loop Cascade Control for an Integrated Electrohydraulic Brake System. IEEE/ASME Transactions on Mechatronics, 25(5), 2460–2471. doi:10.1109/TMECH.2020.2978534.

[39] Montani, M., Vitaliti, D., Capitani, R., & Annicchiarico, C. (2020). Performance review of three car integrated abs types: Development of a tire independent wheel speed control. Energies, 13(23), 6183. doi:10.3390/en13236183.

[40] Kizir, G., & Furkan Kanburoglu, A. (2023). Position Control of External Rotor Permanent Magnet Synchronous Motor with Model Predictive Control. Model Predictive Control - Theory and Applications, IntechOpen, London, United Kingdom. doi:10.5772/intechopen.1001082.

[41] Mechanical Simulation Corporation, Ann Arbor, United States. Available online: https://www.carsim.com (accessed on January 2026).

[42] MATLAB, MathWorks, Natick, United States. Available online: https://www.mathworks.com (accessed on January 2026).

[43] Li, L., Lu, Y., Wang, R., & Chen, J. (2017). A Three-Dimensional Dynamics Control Framework of Vehicle Lateral Stability and Rollover Prevention via Active Braking With MPC. IEEE Transactions on Industrial Electronics, 64(4), 3389–3401. doi:10.1109/TIE.2016.2583400.

[44] Nayereh Raesian Hossein Gholizadeh Narm, ". (2025). A Novel Parallel Control Architecture for Integrated Electro-Hydraulic Brake to Simultaneously Enhance Braking Performance and Vehicle Stability". Automotive Science and Engineering, 15(2), 4739–4754. doi:10.22068/ase.2025.708.